

Effective elasticity of rocks with closely spaced and intersecting cracks

Vladimir Grechka¹ and Mark Kachanov²

ABSTRACT

The noninteraction approximation (NIA) is the simplest effective media theory that describes the overall elasticity of fractured rocks. If the NIA is used for fracture characterization, its accuracy and the range of applicability must be estimated. We do it by performing a series of 3D finite element simulations of effective elasticity for models that contain several sets of fractures embedded in otherwise isotropic host rock. We intentionally place the cracks close to each other to create strong interactions in their local stress fields. In addition, we allow the cracks to intersect in such a way that they do not break a rock specimen apart.

Perhaps surprisingly, we find that fracture interactions and intersections have little influence on the effective elasticity, and the NIA performs well in all cases. While it has a tendency to slightly underestimate the effective stiffnesses, the incurred errors are small; their typical magnitudes are just a few percent in the entire range of the crack densities expected in naturally fractured formations. In our view, this makes the noninteraction approximation the method of choice for fracture characterization.

INTRODUCTION

Theoretical understanding of effective elasticity of rocks containing hydrocarbon-rich cracks is one of the key elements in designing exploration and development programs for naturally fractured reservoirs. This understanding comes from the effective media theories (e.g., Bristow, 1960; Walsh, 1965a, 1965b; Mori and Tanaka, 1973; Budiansky and O'Connell, 1976; Hudson, 1980; Kachanov, 1980; Schoenberg, 1980) that aim at replacing a micro-heterogeneous, fractured rock with a homogeneous one that has the same overall (or effective) elastic properties. The simplest solution to this rather complex problem is called the *noninteraction* approximation (NIA). It places the individual fractures into a re-

motely applied stress field and sums up their contributions to the overall elasticity as if interactions between the fractures did not exist.

Obviously, the NIA not only neglects the interactions but also cannot be applied to intersecting cracks. On the other hand, nature (cores, outcrops, borehole televiewer data) provides abundant examples of both intersecting fracture networks and closely spaced cracks that generate the interacting elastic fields. These well-known observations motivated us to explore whether the NIA can be applied to rocks that contain both interacting and intersecting fractures. Although such applications may seem inappropriate for the noninteraction approximation, there are indications that it might be reasonably accurate. The recent work of Grechka and Kachanov (2006) hints at why this could be the case. While multiple, nonintersecting 3D fracture sets (up to cumulative crack density of 0.14) were characterized by strong local stress and strain interactions, the influence of these interactions on the overall stiffness was negligible by seismic standards (Grechka and Kachanov, 2006).

In this paper, we extend the study of Grechka and Kachanov (2006) by letting the cracks cross each other. Still, their geometrical intersections are expected to have a minor influence on the overall elasticity. We will verify this counterintuitive statement numerically. To do so, we build multiple arrays containing either non-intersecting or both nonintersecting and intersecting cracks and compute the corresponding effective stiffnesses with the finite-element method. We also examine the important issue of the size of the representative-volume element (RVE). Specifically, we show that surprisingly few cracks are needed to produce the effective stiffnesses with an accuracy normally achievable in seismics. In this respect, our work differs from similar studies of Arns et al. (2001, 2002), Saenger and Shapiro (2002), Orlowsky et al. (2003), and Saenger et al. (2004), all of which utilize models containing hundreds or thousands of inclusions.

Since the main goal of our paper is to investigate the influence of interactions and intersections of fractures on the effective elasticity, we limit ourselves to dry cracks because they cause the strongest reduction in the effective stiffness (see Grechka and Kacha-

Manuscript received by the Editor June 30, 2005; revised manuscript received September 6, 2005; published online May 24, 2006.

¹Shell International Exploration and Production, Inc., 3737 Bellaire Blvd., P.O. Box 481, Houston, Texas, 77001-0481. E-mail: vladimir.grechka@shell.com.

²Tufts University, Department of Mechanical Engineering, Medford, Massachusetts 02155. E-mail: mark.kachanov@tufts.edu.

© 2006 Society of Exploration Geophysicists. All rights reserved.

nov, 2006, for the computations involving liquid-filled cracks and Kachanov, 1993, for the underlying theoretical model). Comparison of our numerically generated stiffness tensors with those predicted by the noninteraction approximation reveals that it is sufficiently accurate for the crack densities e expected in naturally fractured reservoirs (typically $e \lesssim 0.1$; e.g., Hudson et al., 1996). We begin our paper with a brief overview of the theoretical results and then present the numerical tests.

NONINTERACTION APPROXIMATION

The effective compliance tensor s_e of a fractured rock is commonly represented as the sum of the background compliance tensor s_b and the contributions $\Delta s^{(k)}$ related to the individual fractures,

$$s_e = s_b + \underbrace{\sum_k \Delta s^{(k)}}_{\Delta s}. \quad (1)$$

Here, the sum is taken with respect to all fractures k in the rock volume V . In the noninteraction approximation (NIA), the individual crack contributions $\Delta s^{(k)}$ are found by assuming that each fracture is subjected to a remotely applied stress and that its interactions with the adjacent fractures can be ignored. The resulting fracture-compliance tensor Δs for dry, penny-shaped cracks, embedded in a purely isotropic host that has zero Poisson's ratio ν_b (or zero Lamé coefficient λ_b), is given by

$$\Delta s_{ijlm} = \frac{2}{3\mu_b} (\alpha_{il}\delta_{jm} + \alpha_{im}\delta_{jl} + \alpha_{jl}\delta_{im} + \alpha_{jm}\delta_{il}), \quad (2)$$

$$(i, j, l, m = 1, 2, 3)$$

(Kachanov, 1980; Sayers and Kachanov, 1995; Schoenberg and Sayers, 1995). In this equation, $\mu_b \neq 0$ is the (nonzero) background Lamé coefficient, δ_{ij} is the Kronecker delta, and α is the symmetric, second-rank crack-density tensor. Equation 2 already accounts for the zero background Poisson's ratio $\nu_b = 0$; that is why the terms corresponding to $\nu_b \neq 0$ are absent there. Tensor α expresses the collective contribution of circular cracks in the form

$$\alpha = \frac{1}{V} \sum_k (a^{(k)})^3 \mathbf{n}^{(k)} \mathbf{n}^{(k)}, \quad (3)$$

where $a^{(k)}$ is the radius of the k th crack, and $\mathbf{n}^{(k)}$ is the unit normal to its face. The trace of tensor α coincides with the usual scalar crack density e ,

$$\text{tr } \alpha = \frac{1}{V} \sum_k (a^{(k)})^3 \equiv e. \quad (4)$$

Therefore, α represents a natural tensorial extension of e to non-random crack orientations and multiple fracture sets.

Because the crack-density tensor α has the second rank, the effective symmetry of fractured media is exactly orthorhombic (or orthotropic) for arbitrarily oriented cracks if $\nu_b = 0$ and approximately orthorhombic (with relatively small errors) if $\nu_b \neq 0$

(Kachanov, 1980, 1993). Numerical simulations of Grechka and Kachanov (2006), performed for a variety of 3D models with non-zero ν_b , confirm this NIA prediction up to the crack density $e = 0.14$. Equations 1 through 3 also indicate that the principal directions of the effective orthotropy coincide with the eigenvectors of α and that the number of independent parameters governing the crack-induced orthotropy is only four, compared to nine for general orthorhombic media (Kachanov, 1980).

If the fractures form L aligned sets with the unit normals $\mathbf{n}^{(\ell)}$ ($\ell = 1, \dots, L$), and each set contains L_ℓ individual fractures, the crack-density tensor given by equation 3 becomes

$$\alpha = \sum_{\ell=1}^L e_\ell \mathbf{n}^{(\ell)} \mathbf{n}^{(\ell)}, \quad (5)$$

where $e_\ell = (1/V) \sum_{k=1}^{L_\ell} (a^{(k)})^3$ is the partial-crack density associated with the ℓ th set. Then, the fracture contribution to the effective compliance is

$$\Delta s_{ijlm} = \frac{2}{3\mu_b} \sum_{\ell=1}^L e_\ell (n_i^{(\ell)} n_l^{(\ell)} \delta_{jm} + n_i^{(\ell)} n_m^{(\ell)} \delta_{jl} + n_j^{(\ell)} n_l^{(\ell)} \delta_{im} + n_j^{(\ell)} n_m^{(\ell)} \delta_{il}), \quad (6)$$

$(i, j, l, m = 1, 2, 3).$

The theory above has been extended to circular crack-like pores that have nonzero aspect ratios $\theta^{(k)}$ (Kachanov et al., 1994). In this case, the fracture contributions to the effective compliance are expressed in terms of Eshelby (1957) tensors $\mathbf{E}^{(k)}$:

$$\Delta s^{(k)} = \phi^{(k)} (\mathbf{J} - \mathbf{E}^{(k)})^{-1} : s_b. \quad (7)$$

Here $\phi^{(k)}$ are the fractions of the total volume occupied by each fracture ($\sum_k \phi^{(k)}$ is usually called the crack porosity), \mathbf{J} is the fourth-rank identity tensor, and the colon denotes a double-dot product (a contraction over two indices).

FINITE-ELEMENT MODELING

To examine the influence of crack interactions and intersections on the effective elasticity, we construct 175 models of fractured media (sometimes called digital rocks) and compute their effective properties with the finite-element method (FEMLAB, 2003). While generally following the methodology outlined by Grechka (2003, 2004), we extend it to diverse (both traction and displacement) boundary conditions. The results below are presented in terms of the stiffness tensors c_e , which are reciprocal to the compliance tensors $c_e = s_e^{-1}$.

Model description

All models discussed in this paper contain three sets of vertical, dry, circular cracks oriented at azimuths $\varphi_1 = 0^\circ$, $\varphi_2 = 30^\circ$, and $\varphi_3 = 40^\circ$ with respect to the horizontal axis x_1 of a global Cartesian coordinate frame. The crack densities of sets two and three are kept fixed at $e_2 = 0.02$ and $e_3 = 0.06$, while the density of set one

changes from $e_1 = 0$ to $e_1 = 0.06$. This allows us to display the effective properties as functions of e_1 . The aspect ratios of cracks vary randomly from 0.04 to 0.08 to simulate their natural variability in rocks.

The host rock in our models is isotropic. Its Lamé coefficient $\mu_b = 6.9$ GPa, while λ_b is deliberately chosen to be zero ($\lambda_b = 0$) to make the effective symmetry exactly orthorhombic (in the NIA) for penny-shaped cracks. As a result, any deviations from the effective orthotropy can be attributed exclusively to the fracture interactions, intersections, and the nonzero aspect ratios. In addition, according to the NIA, the effective stiffness tensors $c_{e,ij}$ (written in Voigt notation) become diagonal for arbitrarily oriented penny-shaped cracks. We will verify this unusual property with 3D numerical simulations. Even though $\lambda_b = 0$ in our models, we expect the conclusions of our study to apply to real rocks that have nonzero λ_b , because its influence on the performance of various effective media theories is known to be mild (e.g., Budiansky and

O'Connell, 1976; Christensen, 1993). Computations of Grechka and Kachanov (2006) performed for $\lambda_b \neq 0$ directly confirm this fact.

The crack arrays used in our finite element computations are also noteworthy because they contain only 10 fractures. We intentionally keep the number of cracks low to illustrate that it is already sufficient (i.e., large enough) to make our models representative given typical accuracy of seismic data.

Nonintersecting cracks

We begin our analysis with cracks that do not cross. The locations of their centers are random (uncorrelated). The cracks are inserted into the model volume V in a sequential manner. A new fracture is accepted only after verification that it does not intersect those already existing ones. Several crack arrays are displayed in Figure 1.

All our simulations exhibit strong interactions in the local stress and strain fields. For example, Figure 2 shows the behavior of the stress component τ_{11} . We emphasize two phenomena which might not be obvious in Figure 2 but, nevertheless, are of key importance for the effective properties. First, as has been noted by Kachanov (1993) and Grechka and Kachanov (2006), the competing effects of stress shielding (blue) and amplification (red) largely cancel each other, leading to a satisfactory accuracy of the noninteraction approximation. Second, the shielding appears to slightly dominate the amplification, implying that interactions tend to stiffen the effective media compared to the predictions of the NIA.

To substantiate and illustrate the above statements, we repeat computations presented in Figure 2 for 40 random realizations of the crack locations at each selected partial-crack density e_1 . The bars in Figure 3 show the 95% confidence intervals of the effective stiffness coefficients $c_{e,ii}$ obtained from our finite-element simulations, while the dots indicate predictions of the NIA (equations 1 and 7). In accordance with our earlier observation, ignoring the crack interactions leads to a slight underestimation of $c_{e,ii}$. The bias of NIA towards softening gradually increases with the crack density, whose total value reaches $e = 0.14$ in our models. Note an inflection in the dependence $c_{e,33}(e_1)$. It is caused by random variations of the crack-aspect ratios $\theta^{(k)}$ and is properly described by the NIA.

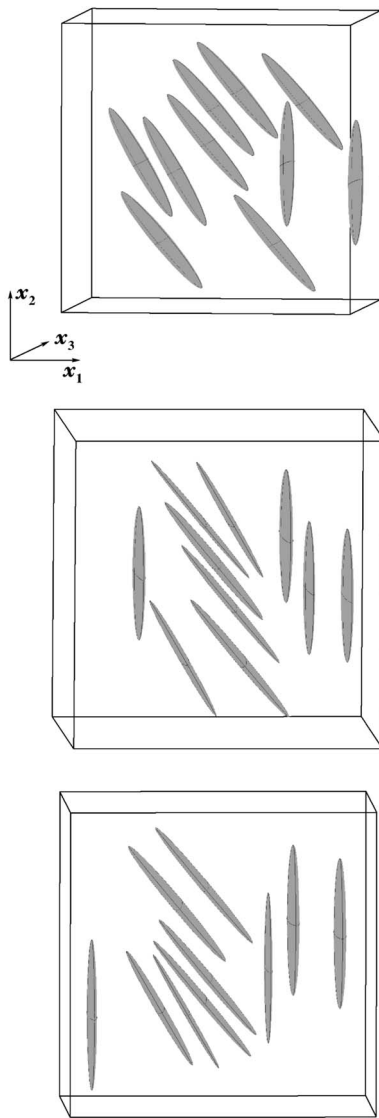


Figure 1. Typical arrays of nonintersecting vertical fractures used in our modeling. The cubes indicate the representative volumes V .

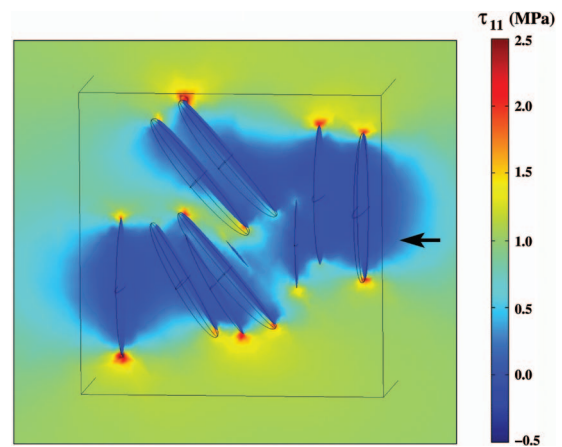


Figure 2. Horizontal cross section of the stress field τ_{11} . The arrow indicates the direction of the uniaxial remote load whose magnitude is equal to 1 MPa.

We observe that the noninteraction approximation has different levels of accuracy for different stiffness components in Figure 3. For instance, $c_{e,11}$, $c_{e,55}$, and especially $c_{e,33}$ are well predicted in the whole range of the crack densities, whereas the accuracy of other stiffness coefficients is somewhat lower. Still, as the bars in Figure 3 correspond to the ranges of admissible stiffness values, the greatest error of the noninteraction approximation is just 3.3% (for $c_{e,22}$ at $e_1 = 0.06$). Such an inaccuracy is too small to be reliably detected and identified from seismic data. For instance, Dewangan and Grechka (2003), who estimated the in-situ stiffnesses from high-quality multicomponent, multiazimuth, walkaway vertical seismic profiling (VSP) measurements, found the stiffness errors to be between 5% and 10%. Thus, we can state that the NIA is sufficiently accurate for seismics, at least when the crack density does not exceed 0.14.

Our conclusions of a good accuracy of the NIA and a slight-stiffening influence of the interactions are in line with those drawn from numerical simulations of 2D crack arrays (Kachanov, 1993; Davis and Knopoff, 1995). On the other hand, the results presented here do not support two popular effective media schemes: self-consistent (Budiansky and O'Connell, 1976) and differential (Va-

vakín and Salganik, 1975). Both schemes predict a softening effect of the interactions; strong according to the self-consistent scheme and moderate according to the differential one.

On the minimum number of cracks needed for simulating effective elasticity

Next, we turn our attention to the scatter of numerical values in Figure 3. The scatter is caused by variations in the interaction patterns from one crack array to another. These variations are always present in models containing any finite number of cracks. This raises a question about the minimum number of fractures that would place c_e into certain predetermined bounds that correspond to the typical measurement errors.

Such a question, which directly relates to the definition of the representative volume element (RVE), was recently discussed by Zohdi and Wriggers (2001) and Kanit et al. (2003). Zohdi and Wriggers (2001) found that only 20 spherical inclusions were needed to obtain the effective bulk modulus K_e and Lamé coefficient μ_e with standard deviations of 0.2% and 1.1%, respectively, in isotropic media with total porosity of 22%. Similar to the results of Zohdi and Wriggers (2001), Figure 3 exhibits different standard

deviations for different $c_{e,ii}$; the greatest standard deviation reaches 3.6% for the stiffness coefficient $c_{e,22}$. All standard deviations, however, again lie well within the inaccuracies expected in the stiffnesses estimated from seismic data. This leads us to an important practical conclusion: Arrays containing as few as 10 cracks are representative for seismics, where errors in the interval stiffness or anisotropic coefficients usually exceed 5%.

Intersecting cracks

So far, our discussion has been limited to the nonintersecting fractures (Figure 1). We now consider circular cracks that cross each other. Their intersections might create intricate fracture geometries ranging from relatively simple X-, 8-, and V-shapes (Figures 4a and 4b) to the more complicated ones shown in Figure 4c. Once we begin dealing with these geometries, our cracks cease to be penny-shaped. Nevertheless, we ignore the intersections and formally apply the NIA (equations 1 and 7) to predict c_e .

Figure 5 gives a visual insight into why the presence of crack intersections can be ignored for the effective stiffnesses. Comparing Figures 2 and 5, we observe that the overall appearance of the fracture-interaction patterns remains virtually unaffected by the crack intersections. Thus, the similarity of Figures 2 and 5 implies that tensors c_e should be close for the models with nonintersecting and intersecting cracks.

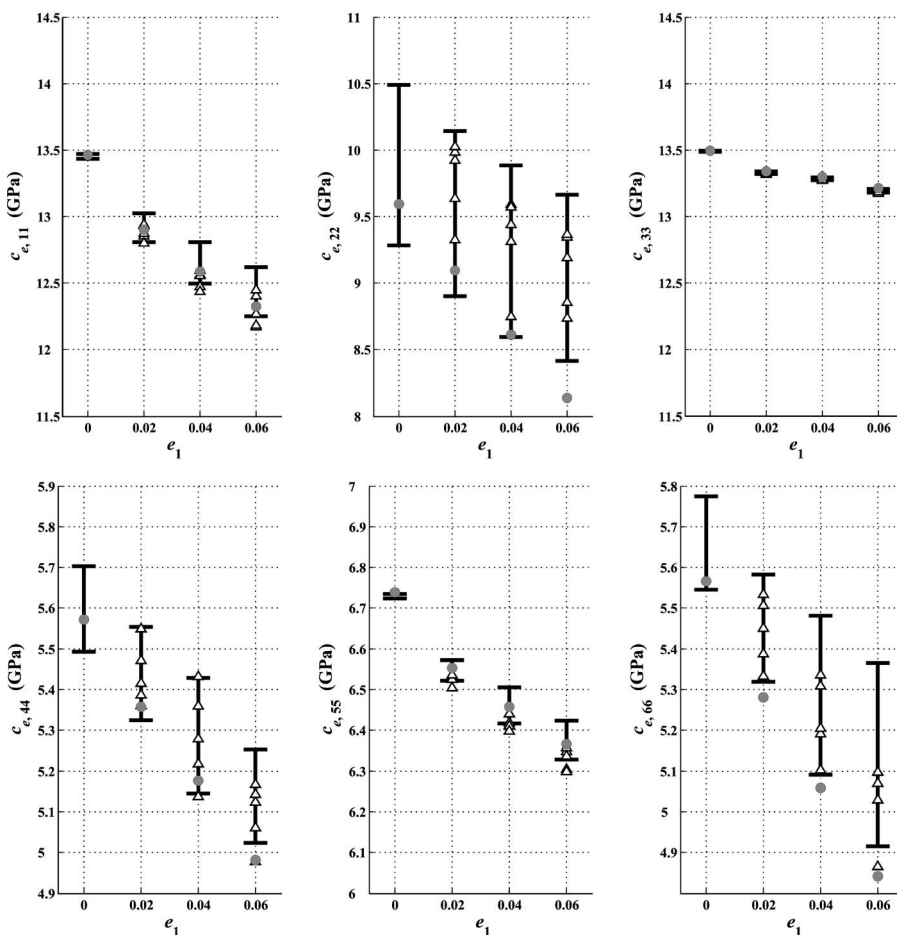


Figure 3. Effective stiffness coefficients $c_{e,ii}$. Bars correspond to the 95% confidence intervals (the mean values ± 2 standard deviations) of the numerically computed stiffness coefficients. Dots are the predictions of the noninteraction approximation (equations 1 and 7). Triangles indicate the stiffnesses for models with intersecting cracks (see below).

Finite element computations of c_e for different arrays of intersecting cracks confirm the above hypothesis. Triangles in Figure 3, which correspond to the models that contain intersecting fractures, usually fall into the ranges of $c_{e,ii}$ (bars) obtained for the models where crack intersections are prohibited. This illustrates the insensitivity of the effective elasticity to the presence of crack intersections and points to a weak interdependence between the overall elastic and fluid-transport properties (see Kachanov and Sevostianov, 2005, for an extended discussion).

Deviation from effective orthotropy

Let us now return to the noninteraction approximation for penny-shaped fractures (equations 1 through 3) that yields vanishing off-diagonal elements of the effective stiffness tensor ($c_{e,ij} = 0$

when $i \neq j$) if $\nu_b = \lambda_b = 0$ and, thus, predicts the effective orthotropy of a special kind. Having computed the effective stiffnesses numerically, we calculate their deviations from diagonal tensors in the ℓ_2 norm:

$$\Delta_e^{\text{diag}} = \frac{\|c_e - c_e^{\text{diag}}\|}{\|c_e\|} \times 100\%, \tag{8}$$

where $\|c\| = \sqrt{\sum_{i,j=1}^6 c_{ij}^2}$ and tensors c_e^{diag} are obtained from c_e by letting

$$c_{e,ij}^{\text{diag}} = \begin{cases} c_{e,ij} & \text{when } i = j \text{ and} \\ 0 & \text{otherwise } (i, j = 1, \dots, 6). \end{cases} \tag{9}$$

Figure 6 displays Δ_e^{diag} for numerically computed effective media (bars and triangles) and compares them with the NIA (equations 1 and 7) that takes into account finite aspect ratios of the fractures (dots). The greatest magnitude of the ℓ_2 norm of off-diagonal components of c_e is only 3%, and almost half of it is because of the nonvanishing fracture openings. Clearly, all tensors c_e are virtually

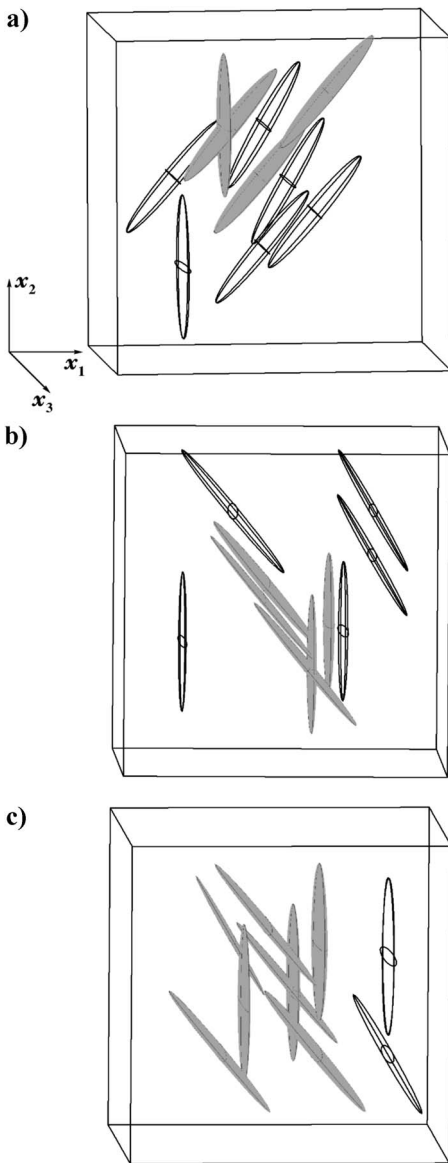


Figure 4. Arrays of intersecting fractures. The crack densities are (a) $e_1 = 0.02$, (b) $e_1 = 0.04$, and (c) $e_1 = 0.06$. Fractures that intersect their neighbors are shaded.

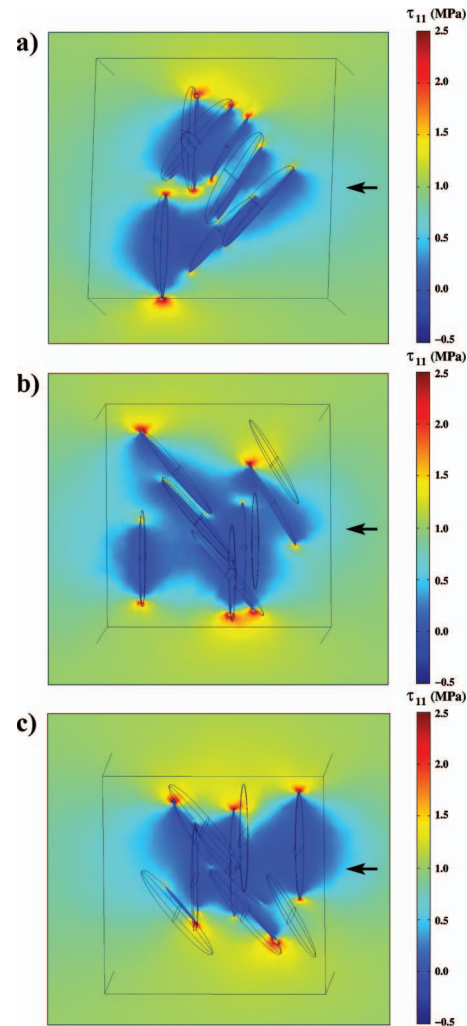


Figure 5. Horizontal cross sections of the stress component τ_{11} for crack arrays shown in Figure 4. Arrows indicate the directions of applied uniaxial remote loads. Their magnitude is 1 MPa.

diagonal, and the approximation of crack-induced orthotropy is well justified. Grechka and Kachanov (2006) drew the same conclusion for models that had nonzero background Lamé coefficient λ_b , which again confirms that a particular value of λ_b has little influence on the overall behavior of cracked media.

DISCUSSION

The noninteraction approximation provides a basic tool for calculating the effective elastic properties of fractured solids. As the word *noninteraction* implies, this approximation should be suitable only to cracks located at such distances from each other that they do not feel the presence of their neighbors. However, the range of applicability of the NIA is actually much wider, primarily because the crack interactions come in the form of stress shielding and amplification that have opposite signs. Therefore, their contributions to effective stiffness tend to cancel each other. As a result, the interactions can be ignored, and the NIA works well not because of their absence, but rather because of their mutual compensation.

The finite element simulations presented in our paper indicate that cancellation of the competing effects of stress shielding and amplification is not complete. For random, uncorrelated crack locations, the shielding slightly dominates the amplification, leading to stiffer effective media than those predicted by the noninteraction approximation. Even though the influence of interactions is noticeable in our computations, they show that the errors of the NIA amount to just a few percent for the crack densities expected in fractured formations. This makes the noninteraction approximation the method of choice for predicting the effective elastic properties of fractured rocks and interpreting seismic data acquired over naturally fractured reservoirs.

We also found that geometrical intersections of fractures do not invalidate the NIA. In fact, the intersections have a minor influence

on the effective properties. We demonstrated this numerically on a number of arrays that had vastly different fracture topologies, ranging from simple X-, 8-, and V-shapes to complicated networks of interconnected cracks. Our computations explicitly proved that such intersections are of no concern for the effective properties in the sense that ignoring them and applying the NIA leads to sufficiently accurate effective results.

CONCLUSIONS

In summary, we have demonstrated the following in this paper: Noninteraction approximation of the effective elastic properties of fractured rocks has an acceptable accuracy for seismic needs, even when the fractures intersect and form interconnected networks. Interactions in the stress and strain fields of the closely spaced cracks tend to stiffen effective media compared to predictions of the noninteraction approximation. The stiffening, however, is small; its magnitude does not exceed a few percent in the range of crack densities ($e \sim 0.1$ or smaller) typical for fractured reservoirs. The symmetry of crack-induced anisotropy is approximately orthorhombic for any orientational distribution of circular, possibly intersecting fractures embedded in otherwise isotropic host rock.

ACKNOWLEDGMENTS

We thank Shell International E & P Inc. for permission to publish this paper. We appreciate many insightful suggestions made by assistant and associate editors of GEOPHYSICS (José Carcione and Boris Gurevich), Valery Levin, and three anonymous reviewers.

REFERENCES

- Arns, C. H., M. A. Knackstedt, and W. V. Pinczewski, 2001, Accurate estimation of transport properties from microtomographic images, *Geophysical Research Letters*, **28**, 3361–3364.
- Arns, C. H., M. A. Knackstedt, W. V. Pinczewski, and E. J. Garboczi, 2002, Computation of linear elastic properties from microtomographic images: Methodology and agreement between theory and experiment, *Geophysics*, **67**, 1396–1405.
- Bristow, J. R., 1960, Microcracks and the static and dynamic elastic constants of annealed and heavily cold-worked metals: *British Journal of Applied Physics*, **11**, 81–85.
- Budiansky, B., and R. J. O'Connell, 1976, Elastic moduli of a cracked solid: *International Journal of Solids and Structures*, **12**, 81–97.
- Christensen, R. M., 1993, Effective properties of composite materials containing voids: *Proceedings of the Royal Society of London*, 440, 461–473.
- Davis, P. M., and L. Knopoff, 1995, The elastic modulus of media containing strongly interacting antiplane cracks: *Journal of Geophysical Research*, **100**, 18,253–18,258.
- Dewangan, P., and V. Grechka, 2003, Inversion of multicomponent, multi-azimuth, walkaway VSP data for the stiffness tensor: *Geophysics*, **68**, 1022–1031.
- Eshelby, J. D., 1957, The determination of the elastic field of an ellipsoidal inclusion and related problems: *Proceedings of the Royal Society of London*, 241, 376–396.
- FEMLAB Reference Manual, 2003, Comsol, available at <http://www.femlab.com>.
- Grechka, V., 2003, Effective media: A forward modeling view: *Geophysics*, **68**, 2055–2062.
- , 2004, Penny-shaped fractures revisited: 74th Annual International Meeting, SEG, Expanded Abstracts, 1694–1697.
- Grechka, V., and M. Kachanov, 2006, Seismic characterization of multiple fracture sets: Does orthotropy suffice?: *Geophysics*, this issue.
- Hudson, J. A., 1980, Overall properties of a cracked solid: *Mathematical Proceedings of Cambridge Philosophical Society*, 88, 371–384.
- Hudson, J. A., E. Liu, and S. Crampin, 1996, The mechanical properties of materials with interconnected cracks and pores: *Geophysical Journal International*, 124, 105–112.

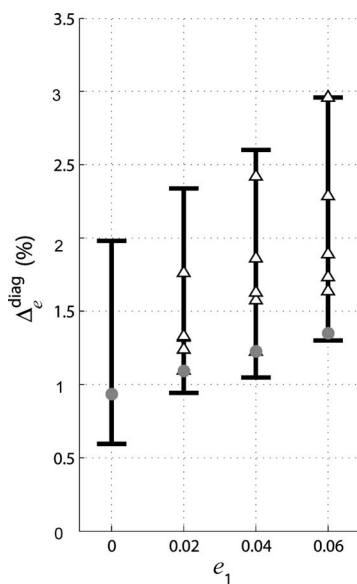


Figure 6. Relative deviations of effective stiffness tensors from diagonal ones. Similar to Figure 3, bars are the 95%-confidence intervals of numerically computed Δ_e^{diag} for nonintersecting crack arrays; triangles are Δ_e^{diag} for models with intersecting cracks, and dots are predictions of the noninteraction approximation (equations 1 and 7).

- Kachanov, M., 1980, Continuum model of medium with cracks: *Journal of the Engineering Mechanics Division*, **106**, 1039–1051.
- , 1993, Elastic solids with many cracks and related problems, in J. W. Hutchinson and T. Wu, eds., *Advances in applied mechanics 30*: Academic Press, 259–445.
- Kachanov, M., and I. Sevostianov, 2005, On quantitative characterization of microstructures and effective properties: *International Journal of Solids and Structures*, **42**, 309–336.
- Kachanov, M., I. Tsurkov, and B. Shafiro, 1994, Effective moduli of solids with cavities of various shapes: *Applied Mechanics Review*, **47**, S151–S174.
- Kanit, T., S. Forest, I. Galliet, V. Mounoury, and D. Jeulin, 2003, Determination of the size of the representative volume element for random composites: Statistical and numerical approach: *International Journal of Solids and Structures*, **40**, 3647–3679.
- Mori, T., and K. Tanaka, 1973, Average stress in matrix and average energy of materials with misfitting inclusions: *Acta Metallurgica*, **21**, 571–574.
- Orlowsky, B., E. H. Saenger, Y. Guéguen, and S. A. Shapiro, 2003, Effects of parallel crack distributions on effective elastic properties — A numerical study: *International Journal of Fracture*, **124**, L171–L178.
- Saenger, E. H., O. S. Krüger, and S. A. Shapiro, 2004, Effective elastic properties of randomly fractured soils: 3D numerical experiments: *Geophysical Prospecting*, **52**, 183–195.
- Saenger, E. H., and S. A. Shapiro, 2002, Effective velocities in fractured media: A numerical study using the rotated staggered finite-difference grid: *Geophysical Prospecting*, **50**, 183–194.
- Sayers, C., and M. Kachanov, 1995, Microcrack-induced elastic wave anisotropy of brittle rocks: *Journal of Geophysical Research*, **100**, 4149–4156.
- Schoenberg, M., 1980, Elastic wave behavior across linear slip interfaces: *Journal of Acoustical Society of America*, **68**, 1516–1521.
- Schoenberg, M., and C. Sayers, 1995, Seismic anisotropy of fractured rock: *Geophysics*, **60**, 204–211.
- Vavakin, A. S., and R. L. Salganik, 1975, Effective characteristics of non-homogeneous media with isolated inhomogeneities: *Mechanics of Solids*, Allerton Press, 58–66.
- Walsh, J. B., 1965a, The effect of cracks on the compressibility of rocks: *Journal of Geophysical Research*, **70**, 381–389.
- , 1965b, The effect of cracks on uniaxial compression of rocks: *Journal of Geophysical Research*, **70**, 399–411.
- Zohdi, T. I., and P. Wriggers, 2001, Aspects of the computational testing of the mechanical properties of microheterogeneous material samples: *International Journal for Numerical Methods in Engineering*, **50**, 2573–2599.